THE JOURNAL OF PHYSICAL CHEMISTRY B

Article

pubs.acs.org/JPCB

Effect of Solvent-Induced Coil to Helix Conformational Change on the Two-Photon Absorption Spectrum of Poly(3,6-phenanthrene)

M. G. Vivas,*[,†] Guy Koeckelberghs,[‡] and C. R. Mendonca*[,†]

[†]Instituto de Física de São Carlos, Universidade de São Paulo, Caixa Postal 369, 13560-970 São Carlos, SP

[‡]Laboratory of Polymer Synthesis, Katholieke Universiteit Leuven, Celestijnenlaan 200F and Celestijnenlaan 200D, B-3001 Heverlee, Belgium

ABSTRACT: This paper investigates the effect of solvent-induced conformational changes of poly(3,6-phenanthrene) on their two-photon absorption (2PA). Such effect was studied employing the wavelength-tunable femtosecond Z-scan technique and modeled using the sum-over-essential states approach. We observed a strong reduction of the 2PA cross-section when the sample was prepared in hexane (poor solvent) in comparison to chloroform (good solvent), which is related to the conformation adopted by the polymer in each case. In chloroform it adopts a random coil conformation, as opposed to the one-handed helix conformation in hexane. Our results pointed out that the coil to helix conformation change decreases the degree of molecular planarity of the polymer π-conjugated backbone, which is primarily responsible for their optical nonlinearity, contributing to diminishing the effective transition dipole moments and, consequently, the 2PA cross-section. Moreover, by studying the nonlinear response with different light polarization, we showed that, although the solvent-induced conformational change does not alter the molecular symmetry of the polymer, it modifies considerably the direction of the transition dipole moments between the excited states.

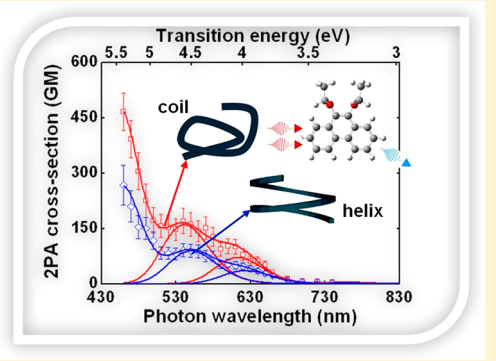

I. INTRODUCTION

Conjugated organic polymers are macromolecules with attractive electrical and optical properties, including electronic conduction,[1] multiphoton emission and absorption,[2−6] nonlinear refractive index,[7] second and third harmonic generation,[8,9] and so on. These properties have been widely studied in the last years due to the prospects of using these materials as active medium in transistors,[10] organic light-emitting,[11] photovoltaic cells[12] and photonic devices.[13,14] Polymers derive their electrical and optical properties mainly from the π-electron delocalization along their chain. Such delocalization can generate high optical polarizabilities, leading to nonlinear optical effects such as intense two-photon absorption (2PA) in the visible and IR regions. However, several intramolecular effects in π-conjugated polymers may contribute to decreasing the linear and nonlinear optical effects, such as, for instance, the decrease of molecular planarity due to the chain folding,[15] weak charge transfer process,[16] and bond length alternation.[17]

2PA is a nonlinear optical process in which two-photons (degenerate or not) are simultaneously absorbed by an atomic or molecular system, promoting an electronic transition between two real energy levels.[18] In this circumstance, the energy difference between the states involved in the transition has to be equal to the sum in energy of the two excitation photons. Consequently, it is possible to promote electronic excitations using photons with lower energy than the optical band gap of the material. However, the probability of this nonlinear optical process to occur is very small and, therefore, it is necessary the use of high light intensity, which nowadays can be delivery by ultrashort laser pulses. A theoretical model widely employed to describe 2PA is the semiclassical second-order time-dependent perturbation theory (TDPT). In this model, the probability of the electronic transition to occur via 2PA is evaluated using the second-order transition matrix elements. According to this theory, the 2PA cross-section is governed by distinct channels that depend basically of the transition dipole moments from ground to excited state ($\vec{\mu}_{g\to e}$), between excited states ($\vec{\mu}_{e\to e'}$) and the permanent dipole moment change ($\Delta\vec{\mu}$). These photophysical parameters, nevertheless, are strongly affected by the surrounding solvent, and consequently, solvent effects may play an important role on the 2PA of organic materials. In general, low polar or nonpolar solvents contribute less to the 2PA cross-section of organic compounds than polar solvents.[19,20] However, such behavior can be altered depending on the molecular structure of the solute.[20]

Conformational changes induced by solvent acts mainly on two aspects, which contribute directly to the 2PA process: the intramolecular charge transfer (ICT) from the terminal groups to the π-bridge and the effective π-bridge conjugation length. Consequently, large modifications in the 2PA cross-section

Received: August 16, 2012
Revised: November 20, 2012
Published: November 26, 2012

magnitude induced by solvent in organic compounds with weak ICT, as the one studied here, are in general associated with large conformational changes undergone by the material.

Recently, Vanormelingen et al.[21] studied the mechanism of solvent action on the conformational steering of poly(3,6-phenanthrene)s (PPh) using linear and nonlinear optical techniques, such as UV−vis, circular dichroism, fluorescence spectroscopy, and hyper-Rayleigh scattering. Among the several results obtained in that work, it is worthwhile mentioning the highly efficient and stable blue emission, even upon annealing, and the solvent-induced conformational changes. PPh adopts a random coil conformation in a good solvent, such as chloroform, and an one-handed helix conformation in poor solvents, like hexane. In this context, here we investigate the influence of solvent-induced coil to helix conformational change on the 2PA properties of PPh. For that, we measured the 2PA cross-section spectrum of PPh in two distinct solvents (chloroform/good solvent and hexane/poor solvent) using the wavelength-tunable femtosecond Z-scan technique. The results were modeled using the sum-over-essential states approach based in the TDPT. Linear optical properties, such as fluorescence lifetime and solvatochromic Stoke shift data, are also reported.

II. EXPERIMENTAL SECTION

All chemicals were of reagent grade and used as supplied (Sigma-Aldrich). The PPh was synthesized and purified as described previously.[21] The PPh molecular structure is illustrated in Figure 1. We prepared PPh/chloroform and

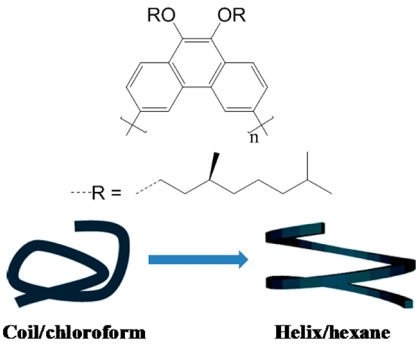

Figure 1. Molecular structure of the poly(3,6-phenanthrene). The picture below shows a representative image of coil to helix conformational changes of PPh in good (chloroform) and poor (hexane) solvents.

hexane solutions with concentrations of 50 μg/mL and 1.5 mg/mL (the concentration for the 2PA measurements was increased from 1.5 to 2.5 mg/mL for wavelengths higher than 660 nm, in order to improve the signal-to-noise ratio), for linear and nonlinear optical measurements, respectively. For the optical measurements the sample was placed in a 2 mm thick quartz cuvette. The steady-state absorption and photoluminescence spectra were recorded using a Shimadzu UV-1800 spectrophotometer and a Perkin-Elmer LS55 fluorimeter, respectively. Nonlinear optical measurements were carried out employing the open aperture Z-scan technique, using 120-fs pulses at 1 kHz repetition rate, delivered by a tunable optical parametric amplifier pumped at 775 nm by a Ti:sapphire chirped pulse amplifier. For each wavelength (460−760 nm), the pulse energy was kept between 40 and 120 nJ with beam waist size ranging from 14 to 17 μm. A Gaussian beam profile was obtained by spatial filtering the excitation beam before the Z-scan setup. A silicon detector was employed to monitor the laser beam intensity in the far-field. To improve the signal-to-noise ratio, we employed the oscillatory Z-scan method, in which the samples is continuously scanned, repeating the experiment several times. Moreover, we used a lock-in amplifier to integrate 1000 shots for each point of the Z-scan signature.

In the open aperture Z-scan technique, 2PA cross-section is determined by translating the sample through the focal plane of a focused Gaussian beam, while transmittance changes in the far field intensity are monitored. For a 2PA process, the light field creates an intensity dependent absorption, $\alpha = \alpha_0 + \beta I$, in which I is the laser beam intensity, α_0 is the linear absorption coefficient, and β is the two-photon absorption coefficient. Far from one-photon resonances, the power transmitted through the sample, for each wavelength, is integrated over time (assuming a pulse with a Gaussian temporal profile) to give the normalized energy transmittance

$$T(z) = \frac{1}{\sqrt{\pi}\, q_0(z, 0)} \int_{-\infty}^{\infty} \ln[1 + q_0(z, 0)\mathrm{e}^{-\tau^2}]\, \mathrm{d}\tau \quad (1)$$

with

$$q_0 = \beta I_0 L(1 + (z^2/z_0{}^2))^{-1} \quad (2)$$

where L is the sample thickness, z_0 is the Rayleigh length, z is the sample position, and I_0 is the laser intensity at the focus. The nonlinear coefficient β is obtained by fitting the Z-scan data with eq 1. The two-photon absorption cross-section, δ_{2PA}, is determined from $\delta_{2PA} = \hbar\omega\beta/N$, where $\hbar\omega$ is the excitation photon energy, and N is the number of molecules per cm^3. Usually the two-photon absorption cross-section is expressed in Göppert-Mayer (GM) units, where 1GM = 1×10^{-50} cm^4 s photon^{-1}.

To measure the fluorescence lifetime of the samples, we doubled the second harmonic of a Q-switched and mode-locked Nd:YAG laser (70 ps) to generate pulses at 266 nm. The 266 nm beam was focused into the sample, placed in a 2 mm-thick fused silica cuvette, with a lens of focal length f = 12 cm. Experimental details about the time-resolved fluorescence setup can be found in ref 4.

III. RESULTS AND DISCUSSION

The steady-state absorption spectrum of the PPh in chloroform (good solvent) solution (solid line) is displayed in Figure 2 (a). Such spectrum presents two absorption bands between 300 and 420 nm (low energy band) and 230−300 nm (high energy band), with molar absorptivity values of approximately 1.7×10^4 and 4.1×10^4 mol^{-1} L cm^{-1}, respectively.

The low energy band is associated with $\pi \rightarrow \pi^*$ transitions from the π-conjugated backbone.[21] The dashed line in Figure 2a exhibits the absorption spectrum obtained when PPh is dissolved in hexane (poor solvent), revealing the effect of lowering the solvent quality. As previously demonstrated by Vanormelingen et al.,[21] the effect of lowering the solvent quality introduces a coil to helix conformational change in the polymer. Such conformational change decreases the molar absorptivity of the low and high energy bands in approximately 30%, as can be observed in Figure 2a. The decrease of the molar absorptivity in hexane indicates a reduction in the molecular planarity of the π-conjugated backbone of the polymer,[4,22] which modify the transition dipole moments from the ground ($|g\rangle$) to the excited state ($|f\rangle$). Such effect can be evaluated using

dx.doi.org/10.1021/jp308161x | J. Phys. Chem. B 2012, 116, 14708−14714

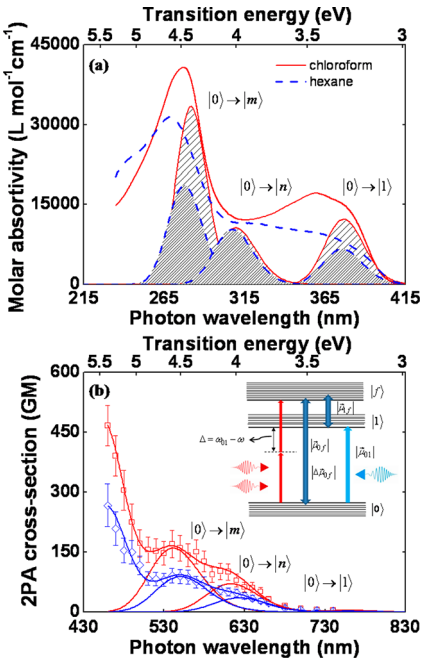

Figure 2. (a) Linear absorption spectra of the PPh dissolved in chloroform (solid line) and hexane (dashed line) solutions. The Gaussian functions represent the energy level adopted in the sum-over-essential approach to model the 2PA spectra. (b) 2PA cross-section spectra of the PPh in chloroform (squares) and hexane (diamonds). The solid lines represent the theoretical fitting obtained employing the sum-over-essential states approach. The inset shows the few-energy level diagram used to model the 2PA spectra.

$$|\vec{\mu}_{gf}| = \sqrt{\frac{3 \times 10^3 \ln(10) hc}{(2\pi)^2 N_A} \frac{n}{L^2} \frac{\varepsilon_{gf}^{max}}{\omega_{gf}} \frac{1}{g_{gf}^{max}}} \quad (3)$$

where ε_{gf}^{max} is the maximum molar absorptivity, N_A is the Avogrado's number, h is Planck's constant, c is the speed of light, ω_{gf} is the transition frequency, and $g_{gf}^{max} = (4 \ln(2)/\pi\Gamma_{gf}^2)^{1/2}$ represents the maximum value of the normalized line width function (assuming Gaussian line-shape) with Γ_{gf} being the damping constant describing full width at half-maximum (FHWM) of the final state line width. $L = 3n^2/(2n^2 + 1)$ is the Onsager local field factor introduced to take into account the medium effect[23] with the refractive index n = 1.490 for chloroform and n = 1.375 for hexane at 20 °C.

By performing semiempirical quantum chemical calculations (data not shown), we observed that the low energy band of PPh can be described mainly by the overlap of three one-photon absorption (1PA) allowed transitions. Thus, the low energy band was fitted by a superposition of three Gaussians. In Figure 2 we show only the Gaussian function that corresponds to the lowest energy transition, which will be subsequently employed to model the nonlinear absorption spectrum, since 2PA data in the range 700−740 nm are related to transitions to the red-edge of the lowest 1PA energy band ($|0\rangle \rightarrow |1\rangle$). Furthermore, for two-photon transition to high energy states (460−700 nm), the long wavelength transition of the 1PA band will be the one with higher contribution to the enhancement effect. Using eq 3 and the Gaussian function illustrated in Figure 2, we determined the transition dipole moment from the ground to the first one-photon allowed excited state as being $|\mu_{01}|^{chlo}$ = 3.0 Debye and $|\mu_{01}|^{hexane}$ = 2.2 Debye. Therefore, the solvent-induced coil to helix conformational change decrease the transition dipole moment from ground to first excited state.

The fluorescence lifetimes of PPh, in both solvents, were measured using 70-ps pulses at 266 nm. The deconvoluted fluorescence decay curves, as well as the lifetime values obtained by using the deconvolution method (in which we considered the response function as Gaussian and a monoexponential function to describe the fluorescence decay) are shown in Figure 3. As it can be seen, the PPh in both

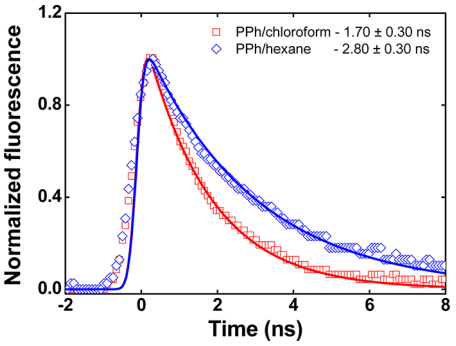

Figure 3. Time-resolved fluorescence for PPh in chloroform (squares) and hexane (diamonds) obtained using 70-ps excitation at 266 nm. The fluorescence lifetime was determined through the deconvolution method, in which we considered the response function as Gaussian to the laser pulse and a monoexponential function to describe the fluorescence decay.

solvents present lifetimes of the order of few nanoseconds, with a slower decay for PPh in hexane (1.70 ± 0.3 ns in chloroform and 2.80 ± 0.3 ns in hexane). These values are in good agreement with the ones obtained for polymers with similar structures.[24]

According to Fermi's Golden rule, the radiative decay rate of dipoles is inversely proportional to the square modulus of the transition dipole moment ($\vec{\mu}_{01}$).[25] Therefore, as the polymer conformation changes from coil to helix,[21] $\vec{\mu}_{01}$ decreases, as previously shown, and the fluorescence lifetime increases as displayed in Figure 3. The decrease in the magnitude of the transition dipole moment and the increase of fluorescence lifetime demonstrates that the coil to helix transition decreases the degree of molecular planarity of the π-conjugated backbone of the polymer.[22]

Figure 2b shows the 2PA spectra of PPh in chloroform (squares) and hexane (diamonds) determined by open-aperture Z-scan measurements with femtosecond pulses. Figure 4 presents some experimental Z-scan curves for the PPh at 560 nm, in both solvents, as well as the corresponding 2PA fit. From Z-scan curves similar to these, at different wavelengths, we determined the 2PA cross-section spectra shown in Figure 2b. However, to obtain the 2PA cross-section value, it is necessary to use high irradiances (in general of the order of GW/cm^2). Therefore, some spurious effects can occur during the measurements as, for example, nonlinear scattering and excited state absorption. Therefore, to confirm the 2PA nature of the experimental results (Figure 2b), we shown in Figure 5 measurements of the dependence of the Z-scan normalized transmittance change (ΔT) as a function of the excitation irradiance at 560 nm (wavelength corresponding to the most intense 2PA allowed band). The slope of approximately 1 obtained from the fit of ΔT as a function of excitation intensity

dx.doi.org/10.1021/jp308161x | J. Phys. Chem. B 2012, 116, 14708−14714

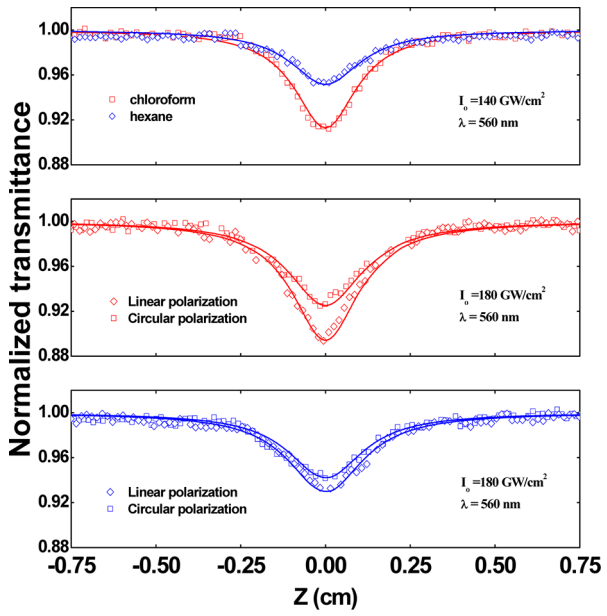

Figure 4. (a) Open-aperture Z-scan curves for PPh in chloroform (squares) and hexane (diamonds) at 560 nm. The solid line represents the fitting employing the eq 1. (b and c) Z-scan curves for PPh in chloroform and hexane, respectively, using the linear and circular polarization light (560 nm).

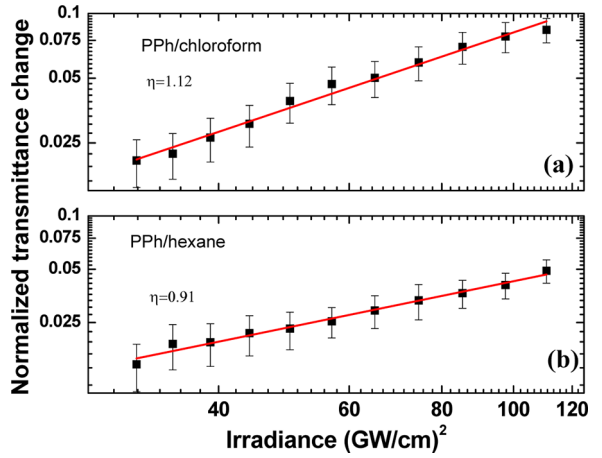

Figure 5. Transmittance change (log−log scale) as a function of pulse irradiance. The slope of approximately 1.0 at 560 nm to the PPh in chloroform (a) and hexane (b) confirms the two-photon nature of the nonlinear process.

(log−log scale) indicates a pure 2PA mechanism, mainly because of three main features of our experimental setup: short pulse duration (120 fs), low repetition rate (1 kHz) and low pulse energy (nJ).

The 2PA spectra of PPh in both solvents (chloroform and hexane) presents the resonance enhancement effect[26,27] below 510 nm, as the excitation wavelength approaches the lowest one-photon allowed state. Furthermore, two 2PA allowed bands, located at 560 and 620 nm, can also be observed in Figure 2b. Although the dipole-electric selection rules are distinct for one- and two-photon absorption process,[28] in noncentrosymmetric molecules such rules can be relaxed.[28] Even though the PPh monomer is centrosymmetric, the polymer does not present such symmetry as revealed by Hyper-Rayleigh scattering measurements.[21] Therefore, the 2PA allowed bands shown in Figure 2b should correspond to electronic transitions which are also 1PA allowed. Such transitions are illustrated by the Gaussian curves in Figure 2a,b ($|0\rangle \rightarrow |1\rangle$, $|0\rangle \rightarrow |n\rangle$, and $|0\rangle \rightarrow |m\rangle$). The 2PA cross-section values, at the peak of the 2PA allowed bands, were determined to be c.a. 160 ± 20 GM at 550 nm and 100 ± 15 GM at 620 nm for PPh in chloroform and 90 ± 15 GM at 550 nm and 50 ± 10 GM at 620 nm for PPh in hexane. A decrease of the 2PA cross-section of *c.a.* 50% is observed due to the solvent-induced coil to helix conformational change. Moreover, the 2PA cross-section values obtained for PPh in both solvents are much smaller than for other conjugated polymers such as MEH-PPV,[29] polyfluorene,[14,30−32] poly(thiophene),[4,33] and poly(phenylene-vinylene).[2,22,34] These results can be explained by the low molecular coplanarity and weak ICT present in PPh, which provide to the polymer a high optical band gap (~3.1 eV).

To further understand the effect of the solvent-induced conformational change on the 2PA spectrum, we used the sum-over-essential states approach to analyze the results of Figure 2b. As polymers, in general, do not present a center of inversion due to their large number of repetitive units, it does not follow the dipole-electric selection rule[28] and, therefore, one- and two-photon transitions are allowed between any electronic states. In this case, we can interpret the 2PA spectrum as consisting of two contributions. The first one (dipolar contribution) corresponds to an electronic transition from ground state to the lowest-energy 2PA allowed state (two-energy level diagram, $|0\rangle \rightarrow |1\rangle$), while the second one, used to model the higher energy states ($|0\rangle \rightarrow |n\rangle$ and $|0\rangle \rightarrow |m\rangle$), uses a three-energy level diagram with one real intermediate energy level ($|1\rangle$). For the dipolar contribution (two-level system), taking into account the average over all possible molecular orientations in an isotropic medium and assuming linearly polarized light and that the dipole moments are parallel, the 2PA cross-section can be written as[35]

$$\delta_{g\rightarrow f}^{(2PA)}(\omega) = \frac{2}{5}\frac{(2\pi)^5}{(nhc)^2} L^4 |\vec{\mu}_{01}|^2 |\Delta\vec{\mu}_{01}|^2 g_{01}(2\omega) \quad (4)$$

where $\Delta\vec{\mu}_{01}$ is the difference between the permanent dipole moments vectors of the excited ($\vec{\mu}_{11}$) and ground ($\vec{\mu}_{00}$) states. $g_{g\rightarrow f}(2\omega)$ represents the line-shape of the excited state, here assumed to be a Gaussian function given by

$$g_{g\rightarrow f}(2\omega) = \sqrt{\frac{4\ln(2)}{\pi\Gamma_{gf}^{\ 2}}}\ \exp\left[-\frac{4\ln(2)}{\Gamma_{gf}^{\ 2}}(2\omega - \omega_{gf})^2\right] \quad (5)$$

where Γ_{gf} is the damping constant describing full width at half-maximum (FHWM) of the final state line width. In eq 4 the damping constants Γ_{01} and transition dipole moment $|\vec{\mu}_{01}|$ can be obtained from linear absorption spectrum and from eq 3, respectively. Moreover, the permanent dipole moment change, $|\Delta\vec{\mu}_{01}|$, can be obtained, in the dipole−dipole interaction, from solvatochromic shift measurements given by

$$|\Delta\vec{\mu}_{01}|^2 = hc\left|\frac{\partial\upsilon}{\partial F}\right| a^3 \quad (6)$$

where $\upsilon = \upsilon_{abs} - \upsilon_{em}$ is the difference between the wavenumber of the maximum fluorescence and absorption (in cm^{-1}). $F(n,\xi) = (\xi - 1)/(2\xi + 1) - (n^2 - 1)/(2n^2 + 1)$ is the Onsager

dx.doi.org/10.1021/jp308161x | J. Phys. Chem. B 2012, 116, 14708−14714

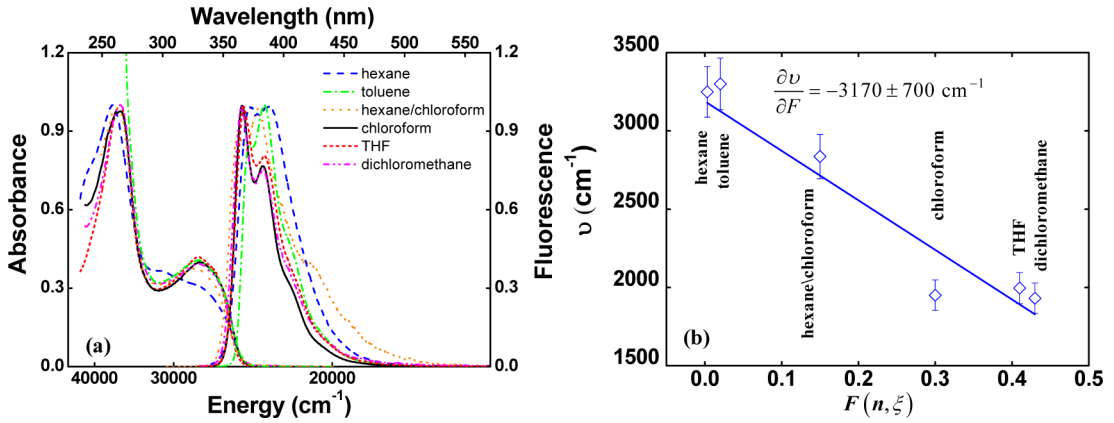

Figure 6. (a) Normalized absorption and fluorescence spectra of the PPh in six different solvents. (b) Solvatochromic Stoke shift (υ) measurements obtained as a function of the Onsager polarity function ($F(n,\xi)$).

polarity function with ξ being the dielectric constant of the solvent. a is the radius of the molecular cavity take as spherical. In general, the parameter a is taken as 40−60% of the π-conjugated backbone maximum length of the molecule.[36] Figure 6a shows the absorption and fluorescence spectra of the PPh in six different solvents, while Figure 6b illustrated the result of the Stokes shift (υ) measurements obtained as a function of the Onsager polarity parameter ($F(n,\xi)$). As it can be seen, we obtained a negative linear slope indicating that the permanent dipole moment from first excited state is smaller than in the ground state ($\vec{\mu}_{11} < \vec{\mu}_{00}$).[37]

Using the result shown in Figure 6 and eq 6 and considering the radius of the molecular cavity as 50% of the π-conjugated backbone maximum length of the monomer (a = 3.3 Å was obtained from the ground state equilibrium geometry), we determined the permanent dipole moment change value as being $|\vec{\mu}_{01}| = 4 \pm 1D$. Using eq 4 and the values obtained for $|\Delta\vec{\mu}_{01}|$ and $|\vec{\mu}_{01}|$ we obtained 2PA cross-section values of 6.5 GM for PPh/chloroform and 3.7 GM for PPh/hexane at 740 nm. These values are in good agreement with the experimental result obtained employing the Z-scan technique (~5.5 GM for chloroform and ~3.0 GM for hexane). The Z-scan curves, corresponding to these values, are displayed in Figure 7.

To model the higher energy 2PA allowed states $|0\rangle \rightarrow |n\rangle$ and $|0\rangle \rightarrow |m\rangle$, located at 560 and 620 nm, respectively, we considered the three-level energy diagram shown in the inset of Figure 2b, that includes the ground state, the first 1PA allowed excited state (intermediate state $|1\rangle$) and one final excited state ($|n\rangle$ or $|m\rangle$). In this approach, we are considering that there is no overlap between the states $|n\rangle$ and $|m\rangle$. Such simplified modeling reduces the complexity of the 2PA cross-section expression, as well as the number of adjustable parameters. Such simplified model describes properly the experimental results, giving a reasonable interpretation to the nonlinear absorption. Therefore, the 2PA cross-section can be written as[35]

$$\delta_{g\rightarrow f}^{(2PA)}(\omega) = \frac{2}{5}\frac{(2\pi)^5}{(nhc)^2}L^4\left\{|\vec{\mu}_{0f}|^2|\Delta\vec{\mu}_{0f}|^2 + R(\omega)|\vec{\mu}_{01}|^2|\vec{\mu}_{1f}|^2 + 2R(\omega)\frac{(\omega_{01}-\omega)}{\omega}|\vec{\mu}_{01}||\vec{\mu}_{1f}||\vec{\mu}_{0f}||\Delta\vec{\mu}_{0f}|\right\} g_{g\rightarrow f}(2\omega) \quad (7)$$

where $\Delta\vec{\mu}_{0f}$ is the difference between the permanent dipole moments vectors of the excited ($\vec{\mu}_{ff}$ with $f = n$ or m) and ground ($\vec{\mu}_{00}$), $\vec{\mu}_{1f}$ is the transition dipole moment between the excited states $|1\rangle \rightarrow |n\rangle$ or $|1\rangle \rightarrow |m\rangle$. For the resonance enhancement factor ($R(\omega) = \omega^2/[(\omega_{01}-\omega)^2+\Gamma_{01}^2(\omega)]$) we assumed that the same intermediate state ($|1\rangle$) contributes to both transitions $|0\rangle \rightarrow |n\rangle$ and $|0\rangle \rightarrow |m\rangle$.[26,27] As it can be seen from eq 7, the 2PA cross-section in a three-energy level system is governed by three contributions: the first corresponds to a 2PA transition in a two-levels system with a change of permanent dipole moment ($\Delta\vec{\mu}_{0f} \neq 0$), while the second contribution corresponds to transitions in a three-level system with one final excited state and one intermediate real excited state ($|1\rangle$), which is responsible for resonance enhancement of the nonlinearity observed below 510 nm. The last contribution corresponds to interference between the two excitation pathways. It is observed that such term decreases as the excitation photon energy approaches the intermediate excited state ($\omega \rightarrow \omega_{01}$).

As can be seen in eq 7, the 2PA cross-section in a three-energy level system depends on the four distinct dipole moments ($|\vec{\mu}_{01}|$, $|\vec{\mu}_{0f}|$, $|\Delta\vec{\mu}_{0f}|$, and $|\vec{\mu}_{1f}|$). The dipole moments $|\vec{\mu}_{01}|$ and $|\vec{\mu}_{0f}|$ can be obtained from eq 3. However, the eq 6 can be applied only to the lowest-energy transition and, therefore, $|\Delta\vec{\mu}_{0f}|$ cannot be obtained directly by it. In this case,

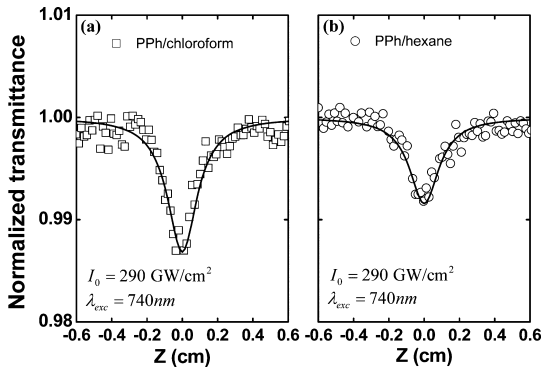

Figure 7. Open-aperture Z-scan curves for PPh in chloroform (a) and hexane (b) at 740 nm. The solid line represents the fitting employing the eq 1.

dx.doi.org/10.1021/jp308161x | J. Phys. Chem. B 2012, 116, 14708−14714

for higher energy transitions, one can use eq 8, which relates the shift of the maximum absorption ($\upsilon_A(\mathrm{cm}^{-1})$) with the solvent polarity ($F(n,\xi)$)[38]

$$\Delta\vec{\mu}_{0f}\cdot\vec{\mu}_{00} = -\mathrm{hc}\frac{\partial\upsilon_{\mathrm{A}}}{\partial F}a^3 \quad (8)$$

where μ_{00} is the permanent dipole moment in the ground state. Using eq 8 and $|\Delta\vec{\mu}_{01}|$ obtained from eq 6, we first obtained $|\vec{\mu}_{00}|$ assuming that the angle between the dipole moments is approximately zero ($|\vec{\mu}_{00}| = 1.6D$). Subsequently, we used this result and the absorption shift data, presented in Figure 8 for

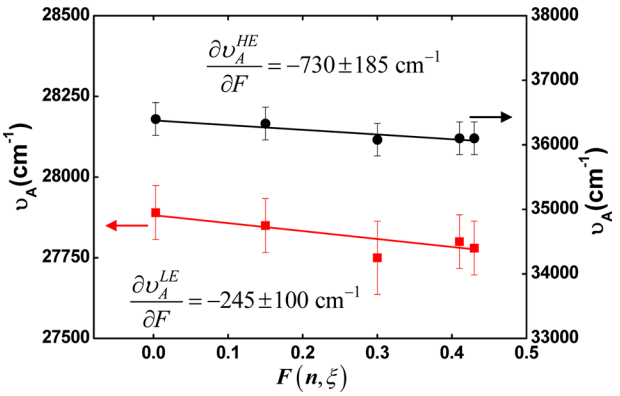

Figure 8. Solvatochromic shift measurements as a function of the Onsager polarity of solvent for the high (HE) and low (LE) energy bands shown in Figure 2a.

the low and high energy bands, to estimate $|\Delta\vec{\mu}_{0f}|$. Using eq 3 and the line width function described by eq 5 and shown in Figure 2 (a), we obtained $|\Delta\vec{\mu}_{0f}|$. Finally, taking into account the 2PA allowed states observed in the nonlinear spectrum and the sum-over-essential states approach, we estimated the transition dipole moments between the excited states $|1\rangle \rightarrow |n\rangle$ and $|1\rangle \rightarrow |m\rangle$ for the PPh in chloroform and hexane. Table 1 shows the spectroscopic parameters obtained using the

Table 1. Spectroscopic Parameters Used/Obtained (Highlight) in/from the Sum-over-Essential States Approach Adopting a Few-Energy-Level Diagram[a]

2PA parameters	PPh/chloroform	PPh/hexane
μ_{00} (Debye)	1.6 ± 0.3	1.6 ± 0.3
$\Delta\mu_{01}$ (Debye)	4.0 ± 1.0	4.0 ± 1.0
μ_{01} (Debye)	3.0 ± 0.5	2.2 ± 0.5
$\Delta\mu_{0n}$ (Debye)	4.5 ± 2.0	4.5 ± 2.0
μ_{0n} (Debye)	3.0 ± 0.5	3.0 ± 0.5
$\Delta\mu_{0m}$ (Debye)	9.0 ± 3.0	9.0 ± 3.0
μ_{0m} (Debye)	5.6 ± 0.5	4.6 ± 0.5
μ_{1n} (Debye)	**11.5 ± 1.0**	**11.5 ± 1.0**
μ_{1m} (Debye)	**10.5 ± 1.0**	**10.5 ± 1.0**

[a]The damping constant describing full width at half-maximum (FWHM) of the final excited state line-shape function (Gaussian function) was estimated in approximately 0.4 eV.

solvatochromic measurements and the ones obtained from the sum-over-essential states approach adopting a few-energy-level diagram (highlight). As can be seen in Table 1, the transition dipole moments between the excited states are equal. However, these results were obtained assuming in eqs 4 and 7 that the dipole moments are parallel, which is not always true for organic compounds, especially when there is a conformational change as reported here. In this context, we estimated the angle between the dipole moments $\vec{\mu}_{01}$ and $\vec{\mu}_{1m}$ by the ratio between the 2PA cross-sections obtained using linearly and circularly polarized light using a two-level system.[39] Figure 4b,c shows the Z-scan curves obtained for PPh in chloroform and hexane solutions using linear and circular polarization light. The 2PA circular/linear ratio, defined as $\Omega_{\mathrm{CLD}} = \sigma_{2\mathrm{PA}}^{\mathrm{CP}}/\sigma_{2\mathrm{PA}}^{\mathrm{LP}}$ is an important parameter for characterizing randomly oriented molecules, because it reveals information about the symmetry of the excited states.[40,41] The values obtained for the 2PA circular/linear ratio were $\Omega_{\mathrm{CLD}} = 0.74$ and $\Omega_{\mathrm{CLD}} = 0.92$ for PPh in chloroform and hexane, respectively. The values of $\Omega_{\mathrm{CLD}} < 1$, indicates that the solvent does not change the polymer excited state symmetry.[40,41] However, the distinct 2PA circular/linear ratio observed for PPh in the distinct solvents can be explained by the alteration in the relative angle between the dipole moments $\vec{\mu}_{01}$ and $\vec{\mu}_{1m}$ from 25° in chloroform to 50° in hexane.[39] Therefore, the change of the solvent (surrounding medium) from chloroform to hexane increase considerably the angle between the transitions dipole moments, indicating that the polymer, in fact, has its molecular geometry modified. Thus, the transition dipole moments presented in Table 1 should be interpreted as effective transition dipole moment, which is a projection of the magnitude of the transition dipole moment modified according to the angle between the two transition dipole moments involved in the transition, given by[42]

$$|\vec{\mu}_{1m}^{\mathrm{eff}}| = |\vec{\mu}_{1m}|\sqrt{\frac{2\cos^2(\theta)+1}{3}} \quad (9)$$

where θ is the angle between the transition dipole moments $\vec{\mu}_{01}$ and $\vec{\mu}_{1m}$. Proceeding of this way, we obtained $|\vec{\mu}_{1m}^{\mathrm{eff}}|^{\mathrm{chlo}} = 9.8D$ and $|\vec{\mu}_{1m}^{\mathrm{eff}}|^{\mathrm{hexane}} = 8.2D$.

IV. FINAL REMARKS

We have studied the solvent-induced conformational change of PPh on their 2PA properties. We observed that the PPh presents 2PA cross-section on the order of few hundreds of Göppert-Mayer units and that this value decreases sharply (about 50%) when the polymer undergoes a conformational change from coil (in chloroform) to helix (in hexane). On the other hand, we did not verify major changes in the spectral behavior of the 2PA due to the solvent. Using the polarized femtosecond Z-scan technique we found that, although the magnitude of the transition dipole moments between the excited states ($|1\rangle$ and $|m\rangle$) are not greatly affect by the solvent, the relative angle between them is. In chloroform we obtained an angle between $\vec{\mu}_{01}$ and $\vec{\mu}_{1m}$ of about 25°, whereas in hexane such an angle is 50° because of the coil to helix conformational change. Furthermore, from solvatochromic Stoke shift measurements, we observe that the PPh presents a permanent dipole moment of the excited state that is smaller than the ground state one. As a final remark, our results indicate that the quality of solvent modifies mostly the ground state of the polymer, altering strongly their linear and nonlinear absorption properties.

AUTHOR INFORMATION

Corresponding Author

*E-mail: mavivas82@yahoo.com.br; crmendon@ifsc.usp.br.

Notes

The authors declare no competing financial interest.

■ ACKNOWLEDGMENTS

Financial support from FAPESP (Fundação de Amparo à Pesquisa do estado de São Paulo), CNPq (Conselho Nacional de Desenvolvimento Científico e Tecnológico), Coordenação de Aperfeiçoamento de Pessoal de Nível Superior (CAPES), and the Air Force Office of Scientific Research is acknowledged. Technical assistance from André L. S. Romero is gratefully acknowledged.

■ REFERENCES

(1) Barford, W. *Electronic and Optical Properties of Conjugated Polymers*; Oxford Science Publications: Sheffield, U.K., 2005.
(2) Chung, S. J.; Rumi, M.; Alain, V.; Barlow, S.; Perry, J. W.; Marder, S. R. *J. Am. Chem. Soc.* **2005**, *127*, 10844−10845.
(3) Correa, D. S.; De Boni, L.; Balogh, D. T.; Mendonca, C. R. *Adv. Mater.* **2007**, *19*, 2653−2656.
(4) Vivas, M. G.; Nogueira, S. L.; Silva, H. S.; Neto, N. M. B.; Marletta, A.; Serein-Spirau, F.; Lois, S.; Jarrosson, T.; De Boni, L.; Silva, R. A.; et al. *J. Phys. Chem. B* **2011**, *115*, 12687−12693.
(5) Oliveira, S. L.; Correa, D. S.; De Boni, L.; Misoguti, L.; Zilio, S. C.; Mendonca, C. R. *Appl. Phys. Lett.* **2006**, *88*, 021911.
(6) Ferreira, P. H. D.; Vivas, M. G.; De Boni, L.; dos Santos, D. S.; Balogh, D. T.; Misoguti, L.; Mendonca, C. R. *Opt. Express* **2012**, *20*, 518−523.
(7) Jang, J. I.; Mani, S.; Ketterson, J. B.; Lovera, P.; Redmond, G. *Appl. Phys. Lett.* **2009**, *95*, 211906.
(8) Cho, M. J.; Choi, D. H.; Sullivan, P. A.; Akelaitis, A. J. P.; Dalton, L. R. *Prog. Polym. Sci.* **2008**, *33*, 1013−1058.
(9) Schaller, R. D.; Snee, P. T.; Johnson, J. C.; Lee, L. F.; Wilson, K. R.; Haber, L. H.; Saykally, R. J.; Nguyen, T. Q.; Schwartz, B. J. *J. Chem. Phys.* **2002**, *117*, 6688−6698.
(10) Ong, K. H.; Lim, S. L.; Tan, H. S.; Wong, H. K.; Li, J.; Ma, Z.; Moh, L. C. H.; Lim, S. H.; De Mello, J. C.; Chen, Z. K. *Adv. Mater.* **2011**, *23*, 1409−1413.
(11) Chen, S. F.; Deng, L. L.; Xie, J.; Peng, L.; Xie, L. H.; Fan, Q. L.; Huang, W. *Adv. Mater.* **2010**, *22*, 5227−5239.
(12) Boudreault, P. L. T.; Najari, A.; Leclerc, M. *Chem. Mater.* **2011**, *23*, 456−469.
(13) Bader, M. A.; Marowsky, G.; Bahtiar, A.; Koynov, K.; Bubeck, C.; Tillmann, H.; Horhold, H. H.; Pereira, S. *J. Opt. Soc. Am. B* **2002**, *19*, 2250−2262.
(14) Correa, D. S.; De Boni, L.; Nowacki, B.; Grova, I.; Fontes, B. D.; Rodrigues, P. C.; Tozoni, J. R.; Akcelrud, L.; Mendonca, C. R. *J. Polym. Sci., Part B: Polym. Phys.* **2012**, *50*, 148−153.
(15) Bounos, G.; Ghosh, S.; Lee, A. K.; Plunkett, K. N.; DuBay, K. H.; Bolinger, J. C.; Zhang, R.; Friesner, R. A.; Nuckolls, C.; Reichman, D. R.; et al. *J. Am. Chem. Soc.* **2011**, *133*, 10155−10160.
(16) Simas, E. R.; Gehlen, M. H.; Pinto, M. F. S.; Siqueira, J.; Misoguti, L. *J. Phys. Chem. A* **2010**, *114*, 12384−12390.
(17) GarciaBach, M. A.; Valenti, R.; Klein, D. J. *Phys. Rev. B* **1997**, *56*, 1751−1761.
(18) Goeppert-Mayer, M. *Ann. Phys.* **1931**, *8*, 273−294.
(19) Wang, C. K.; Zhao, K.; Su, Y.; Ren, Y.; Zhao, X.; Luo, Y. *J. Chem. Phys.* **2003**, *119*, 1208−1213.
(20) He, G. S.; Tan, L. S.; Zheng, Q.; Prasad, P. N. *Chem. Rev.* **2008**, *108*, 1245−1330.
(21) Vanormelingen, W.; Smeets, A.; Franz, E.; Asselberghs, I.; Clays, K.; Verbiest, T.; Koeckelberghs, G. *Macromolecules* **2009**, *42*, 4282−4287.
(22) Johnsen, M.; Paterson, M. J.; Arnbjerg, J.; Christiansen, O.; Nielsen, C. B.; Jørgensenb, M.; Ogilby, P. R. *Phys. Chem. Chem. Phys.* **2008**, *10*, 1177−1191.
(23) Onsager, L. *J. Am. Chem. Soc.* **1936**, *58*, 1486−1493.
(24) Chen, Y. C.; Wang, Z. M.; Yan, M. D.; Prahl, S. A. *Luminescence* **2006**, *21*, 7−14.
(25) Loudon, R. *The Quantum Theory of Light*, 3rd ed.; Clarendon Press: Oxford, U.K., 2003.
(26) Kamada, K.; Ohta, K.; Iwase, Y.; Kondo, K. *Chem. Phys. Lett.* **2003**, *372*, 386−393.
(27) Vivas, M. G.; Piovesan, E.; Silva, D. L.; Cooper, T. M.; De Boni, L.; Mendonca, C. R. *Opt. Mater. Express* **2011**, *1*, 700−710.
(28) Bonin, K. D.; McIlrath, T. J. *J. Opt. Soc. Am. B* **1984**, *1*, 52−55.
(29) De Boni, L.; Andrade, A. A.; Correa, D. S.; Balogh, D. T.; Zilio, S. C.; Misoguti, L.; Mendonca, C. R. *J. Phys. Chem. B* **2004**, *108*, 5221−5224.
(30) Belfield, K. D.; Morales, A. R.; Hales, J. M.; Hagan, D. J.; Van Stryland, E. W.; Chapela, V. M.; Percino, J. *Chem. Mater.* **2004**, *16*, 2267−2273.
(31) Belfield, K. D.; Morales, A. R.; Kang, B. S.; Hales, J. M.; Hagan, D. J.; Van Stryland, E. W.; Chapela, V. M.; Percino, J. *Chem. Mater.* **2004**, *16*, 4634−4641.
(32) Tong, M.; Sheng, C. X.; Vardeny, Z. V. *Phys. Rev. B* **2007**, *75*, 125207.
(33) Belfield, K. D.; Andrade, C. D.; Yanez, C. O.; Bondar, M. V.; Hernandez, F. E.; Przhonska, O. V. *J. Phys. Chem. B* **2010**, *114*, 14087−14095.
(34) Nielsen, C. B.; Arnbjerg, J.; Johnsen, M.; Jorgensen, M.; Ogilby, P. R. *J. Org. Chem.* **2009**, *74*, 9094−9104.
(35) Meath, W. J.; Power, E. A. *J. Phys. B* **1984**, *17*, 763−781.
(36) Guilbault, G. G. *Practical Fluorescence: Theory, Methods, and Techniques*; New York, 1973.
(37) Reichardt, C. *Chem. Rev.* **1994**, *94*, 2319−2358.
(38) Drobizhev, M.; Makarov, N. S.; Rebane, A.; de la Torre, G.; Torres, T. *J. Phys. Chem. C* **2008**, *112*, 848−859.
(39) Vivas, M. G.; De Boni, L.; Bretonniere, Y.; Andraud, C.; Mendonca, C. R. *Opt. Express* **2012**, *20*, 18600−18608.
(40) Nascimento, M. A. C. *Chem. Phys.* **1983**, *74*, 51−66.
(41) Tinoco, I. *J. Chem. Phys.* **1975**, *62*, 1006−1009.
(42) Cronstrand, P.; Luo, Y.; Agren, H. *J. Chem. Phys.* **2002**, *117*, 11102−11106.